Lysine Carboxylation in Proteins: OXA-10 β-Lactamase

Jie Li,[1] Jason B. Cross,[1] Thom Vreven,[3] Samy O. Meroueh,[2] Shahriar Mobashery,[2] and H. Bernhard Schlegel[1,3*]

[1]*Department of Chemistry and Institute for Scientific Computing, Wayne State University, Detroit, Michigan*
[2]*Department of Chemistry and Biochemistry, University of Notre Dame, Notre Dame, Indiana*
[3]*Gaussian, Inc., 340 Quinnipiac St Bldg 40, Wallingford, Connecticut*

ABSTRACT   An increasing number of proteins are being shown to have an N_ζ-carboxylated lysine in their structures, a posttranslational modification of proteins that proceeds without the intervention of a specific enzyme. The role of the carboxylated lysine in these proteins is typically structural (hydrogen bonding or metal coordination). However, carboxylated lysines in the active sites of OXA-10 and OXA-1 β-lactamases and the sensor domain of BlaR signal-transducer protein serve in proton transfer events required for the functions of these proteins. These examples demonstrate the utility of this unusual amino acid in acid-base chemistry, in expansion of function beyond those of the 20 standard amino acids. In this study, the ONIOM quantum-mechanical/molecular-mechanical (QM/MM) method is used to study the carboxylation of lysine in the OXA-10 β-lactamase. Lys-70 and the active site of the OXA-10 β-lactamase were treated with B3LYP/6-31G(d,p) density functional calculations and the remainder of the enzyme with the AMBER molecular mechanics force field. The barriers for unassisted carboxylation of neutral lysine by carbon dioxide or bicarbonate are high. However, when the reaction with CO_2 is catalyzed by a molecule of water in the active site, it is exothermic by about 13 kcal/mol, with a barrier of approximately 14 kcal/mol. The calculations show that the carboxylation and decarboxylation of Lys-70 are likely to be accompanied by deprotonation and protonation of the carbamate, respectively. The analysis may also be relevant for other proteins with carboxylated lysines, a feature that may be more common in nature than previously appreciated. Proteins 2005; 61:246–257.   © 2005 Wiley-Liss, Inc.

Key words: penicillin-binding proteins; class D β-lactamase; carboxylation mechanism; ONIOM QM/MM method; density functional calculations

INTRODUCTION

Carboxylated lysine residues have been observed in about a dozen or so proteins.[1–6] This unusual amino acid is typically involved in structural functions, such as hydrogen bonding to the protein or coordination to metal ions. In contrast to such structural roles, carboxylated lysine has been shown to have an essential mechanistic function in the class D β-lactamase OXA-10 from *Pseudomonas aerugi-*

nosa.[4] It has also been observed in the catalytic site of OXA-1 β-lactamase from *Escherichia coli*.[6] More recently, a carboxylated lysine has been implicated in the reaction of the β-lactam sensor domain of the BlaR signal transducer protein from *Staphylococcus aureus*.[5,7] The carboxylated lysine removes a proton from the side chain of the active-site serine of the class D β-lactamases and the BlaR protein, promoting its acylation by the substrate. The same carboxylated lysine activates a water molecule in the second step of the catalytic process in β-lactamases, which involves deacylation of the acyl-enzyme species. In the BlaR protein, decarboxylation traps the acyl-enzyme complex, ensuring signal sensing and message transduction.[5,7] The involvement of the carboxylated lysine in the mechanisms of these proteins is an excellent example of how evolutionary forces have expanded the repertoire of the side-chain functionalities beyond the twenty commonly found amino acids.

The class D OXA β-lactamases are members of the family of bacterial resistance enzymes that have evolved to destroy β-lactam antibiotics.[8,9] Class D β-lactamases confer high levels of resistance to a broad spectrum of β-lactam antibiotics, but are the least understood[6] of this family of enzymes. The X-ray crystal structures of the OXA-10[4] and OXA-1[6] β-lactamases have recently been solved. The asymmetric unit cell of the former consists of two equivalent dimers, while the latter has a unit cell with two equivalent monomers. Lys-70 is carboxylated in both proteins; in contrast, the corresponding lysines in the active sites of class A and class C β-lactamases are not carboxylated. Previously, carboxylated lysine residues have been found to occur in D-ribulose-1,5-bisphosphate carboxylase/oxygenase (rubisco),[10] in urease from *Klebsiella aerogenes*,[1] and in phosphotriesterase from *Pseudomonas*

---

diminuta,[11] along with a few other proteins,[12,13] but in these cases the carbamate is stabilized by interactions with metal cations and/or it serves a structural role.[1-3] The carboxylated Lys-70 of the OXA-1 and OXA-10 β-lactamases are not coordinated to a metal ion.

The lysine in the active site of class D β-lactamases sits in a hydrophobic pocket that should favor the free base form when not carboxylated.[14] This deduction is supported by Poisson–Boltzmann calculations, which indicate that the active-site lysine has a much lower pK_a than the equivalent lysine in the active site of class A β-lactamase TEM.[15] Specifically, the calculated pK_a values of Lys-70 in the uncarboxylated form of OXA-10 are 6.8 and 7.0 for the non-equivalent monomers. The hydrophobic environment should also favor carboxylation by carbon dioxide rather than by bicarbonate. The carboxylate group of the carboxylated lysine is stabilized by hydrogen bonding interactions with Ser-67 O_γ, by the side chain nitrogen of Trp-154, and by a crystallographic water molecule.[4] The crystal structure of the OXA-10 β-lactamase has been examined at four different pH values: 6.0, 6.5, 7.5, and 8.5.[16] One subunit of each dimer was carboxylated at all pH values studied; the other subunit was carboxylated at high pH but decarboxylated at low pH.

Studies with $^{14}CO_2$ and $^{13}CO_2$ showed that carboxylation in OXA-10 is reversible and essential for catalytic activity.[16] The fully decarboxylated form is inactive, and the degree of carboxylation (as measured by the uptake of $^{14}CO_2$) correlates with the degree of recovery of activity. Independent nuclear magnetic resonance (NMR) experiments with $^{13}CO_2$ confirmed the presence of a carboxylated lysine in the active enzyme.[16] The mechanistic role of carboxylated Lys-70 is further supported by the fact that the Lys-70-Ala mutant is entirely inactive.

The dissociation constant for CO_2 in OXA-10 enzyme was measured to be in the micromolar to submicromolar range (K_D = 12.4 ± 0.01 μM for the monomeric form, K_D = 0.23 ± 0.05 μM for the dimer).[16] The *in vivo* concentration of CO_2 has been reported at 1.3 mM,[17] indicating that Lys-70 is fully carboxylated in its native state. Under certain conditions, the OXA-10 β-lactamase shows biphasic kinetics, with an initially high reaction rate followed by a slower one. Earlier studies attributed this to a dimer/monomer equilibrium.[18,19] However, recent work has shown that the biphasic kinetics of the monomer simplify to monophasic upon the addition of excess bicarbonate as a source of carbon dioxide. This suggests that the second and slower phase is associated with decarboxylation of lysine during the course of catalysis, a process that has to be reversed for catalysis to resume and reach its conclusion.[16] Since carboxylation/decarboxylation is crucial to understanding the activity of the OXA-10 β-lactamase and other enzymes that would use carboxylated lysines in their catalytic mechanism, we have undertaken the first computational study of this process using a mixed quantum/molecular (classical) (QM/MM) approach.

QM/MM methods are valuable tools for computational investigations of biologically interesting molecules.[20-22] Although classical force-field calculations work well for investigating the dynamics and non-covalent binding of biomolecules, they are of limited use in describing chemical reactions, since parameters are not defined for transition structures in which bonds are partially formed. Molecular orbital (MO) calculations can describe transition structures well, but they are computationally expensive, and only a small portion of the biomolecule can be treated at the quantum level. Studying enzymes by MO methods would necessitate the removal of most of the protein from the model system. This may eliminate the structural framework required to keep the active site aligned properly for the enzymatic process,[23] and it could also remove necessary electrostatic interactions that play an important role in catalysis. QM/MM techniques can employ the strengths of both of these approaches. The active-site region can be treated using high-level molecular orbital theory, while the more distant parts of the enzyme can be treated using low-cost molecular mechanics. In this study, we have used the ONIOM QM/MM method[24-26] to study the energetics of carboxylation of Lys-70 in the OXA-10 β-lactamase. The findings reported herein have direct implications for other enzymes that possess carboxylated lysine residues in their structures and should be of general interest.

MATERIALS AND METHODS

Molecular orbital calculations were carried out using a development version of the GAUSSIAN series of programs.[27] Optimized geometries for the gas phase reactions were computed using the Hartree–Fock,[28] MP2,[29,30] and B3LYP[31-33] levels of theory, with the 6-31G(d),[34,35] 6-31G(d,p)[34,35] and 6-311G(d,p) basis sets.[36,37] High-accuracy energies were computed using the CBS–APNO method,[38] which uses QCISD/6-311G(d,p)-optimized geometries[39] and several higher-order corrections to the energy.[38] Solvation effects were included using the conductor-like polarizable continuum model (CPCM).[40]

The high-resolution (1.39 Å) structure of the OXA-10 β-lactamase was obtained from the Research Collaboratory for Structure Bioinformatics database (RCSB; http://www.rcsb.org/pdb/index.html) with accession number 1K55. Manipulation of the structure was carried out with the Sybyl 6.7 package.[41] The enzyme was protonated using the program Protonate, part of the AMBER 6 suite of programs,[42] and corresponds to pH7 for the standard residues. Force-field parameters and atomic charges for standard protein residues were obtained from the "parm99" set of parameters.[43] Atomic charges of the carboxylated lysine were computed using the restrained electrostatic potential (RESP) fitting procedure.[44] A HF/6-31G(d) single-point energy calculation was used to determine the electrostatic potential around the molecule, which was subsequently employed in the two-stage RESP fitting procedure. No counterions were added, and electrostatics were calculated using particle mesh Ewald (PME).[45] The protein was then immersed in a box of TIP3P water with at least 10 Å between any face of the box and the enzyme, resulting in a box with dimensions of 84 × 77 × 76 Å. The solvated enzyme system consisted of 31,270 atoms. Water mol-

ecules were equilibrated by running a 30-ps molecular dynamics simulation while holding the protein fixed, which was followed by 20,000 steps of conjugate-gradient energy minimization of the entire system. The resulting structure was then used to prepare the system for QM/MM calculations by extracting the solute and all water molecules within 12 Å of the carboxylated lysine and 3 Å of any other residues. To confirm the presence of a key non-crystallographic water found in the active site during the equilibration, the system was also subjected to 2 ns of molecular dynamics simulations. The simulation was carried out using PME electrostatics[45] and the SHAKE algorithm,[46] which afforded the use of a 2-fs time step. The evolution of the root mean square deviation from the X-ray structure over the course of the trajectory is shown in Figure 1 of the Supplementary Material, revealing that the protein is fully equilibrated after 500 ps of molecular dynamics. The radial distribution function for the water–carbamate oxygen distance was computed for the subsequent 1.5 ns of the simulation (Fig. 2 of the Supplementary Material). The large peak at 2.8 Å confirms the continued presence of a water molecule within hydrogen-bonding distance of the carbamate oxygen over the course of the trajectory and validates the use of the equilibrated structure for the QM/MM calculations.

The two-layer ONIOM method[24,25] with electrostatic embedding[47] was used for mixed QM/MM calculations. This method divides the calculation of the enzyme system into a QM computation in a model region and MM calculations on both the real system and the model region.

$$E_{\text{real}}^{ONIOM} = E_{\text{real}}^{MM} - E_{\text{model}}^{MM} + E_{\text{model}}^{QM} \qquad (1)$$

Link atoms are used to cap any bonds that are cut in forming the model region. The quantum calculations on the model system were carried out at the B3LYP/6-31G(d,p) level of theory, which is generally more accurate than BLYP density functional calculations and more affordable than MP2 calculations. The AMBER force field was used for the molecular mechanics computations. The Gaussian code uses the "parm96" set of parameters,[48] but this should not affect the results. The partial charges are the same as in "parm99," and the differences in parameters for bonded atoms have very small effects because most of the MM region of the protein is held fixed in the ONIOM calculations. Although the AMBER force field cannot describe the transition states, this does not cause difficulties when the force field is used as the low level in an ONIOM calculation. The distorted bonds in the transition state contribute equally to the low-level calculations on the model system ($E_{\text{model}}^{\text{MM}}$) and the real system ($E_{\text{real}}^{\text{MM}}$), and these contributions cancel exactly when differences are taken in computing the ONIOM energy using eq. (1). Electrostatic embedding allows the wavefunction of the quantum layer to be influenced by the electrostatic field of the classical layer, using the partial charges defined in the AMBER force field. Both the MM and the QM calculations on the model system are calculated in the presence of these charges. A covalent bond at the interface between the two layers required special consideration. In this circum-

stance, large MM charges close to the QM region may cause overpolarization of the wavefunction. This problem is overcome by scaling the MM embedding charges to zero for atoms less than four bonds from the QM region. Because this scaling is done for the charges in both the QM model system and the MM model system, the total charge interaction is balanced (for a more detailed discussion, see ref. 26). In addition, the link atoms added to the model system were assigned a charge of zero.

In QM/MM calculations, the C_δ, C_ϵ, and N_ζ atoms (and associated H atoms) of the Lys-70 side chain, as well as the atoms of the CO_2 or HCO_3^- molecule with and without a catalytic water, C_α, C_β, and O_γ of Ser-67, methylindole for the side chain of Trp-154, and a crystallographically conserved water molecule, were incorporated into the quantum layer. An additional water molecule, which was found to be conserved over the course of a 2-ns molecular dynamics simulation, was included in the active site for carboxylation by CO_2 but not for HCO_3^-. The rest of the protein was held fixed in Cartesian space at its equilibrated geometry. Since the carboxylation reaction takes place in a localized part of the enzyme, this reduced the numerical noise in the relative energies due to conformational changes at a distance from the active site.

RESULTS AND DISCUSSION

The investigation of lysine carboxylation in the OXA-10 β-lactamase involved several stages. First, the analogous small-molecule reactions were studied in the gas phase to determine what level of theory in the quantum region is sufficient to describe the chemistry with acceptable accuracy, yet efficient enough to be practical in the QM/MM calculations. The gas-phase carboxylation of methylamine was chosen for this purpose, since methylamine is the smallest model compound that can adequately mimic the lysine side chain. Carboxylation by both CO_2 and HCO_3^- were considered. Because the barriers for the proton transfer involved in the gas phase carboxylation are rather high, we explored the possibility of a molecule of water participating in the proton relay. Then, to assess the importance of environmental effects, a simple solvation model was included in addition to the catalytic water molecule. Finally, carboxylation of Lys-70 within the active site of the OXA-10 β-lactamase was studied with the ONIOM QM/MM method. Reactions with both carbon dioxide and bicarbonate were examined with and without the participation of a water molecule.

Carboxylation of Methylamine in Gas Phase

The carboxylation of amines has been of interest for over a century.[49] More recently, the interaction of CO_2 with ionic liquids containing amine groups has attracted considerable attention in connection with gas purification.[50–57] Nevertheless, physical chemical data on the gas-phase carboxylation of simple amines are limited. A number of theoretical studies indicate that the carboxylation of amines by CO_2 involves high barriers associated with 1,3 proton transfers.[56,58] Although early experimental literature suggested a zwitterionic intermediate in aqueous solution,
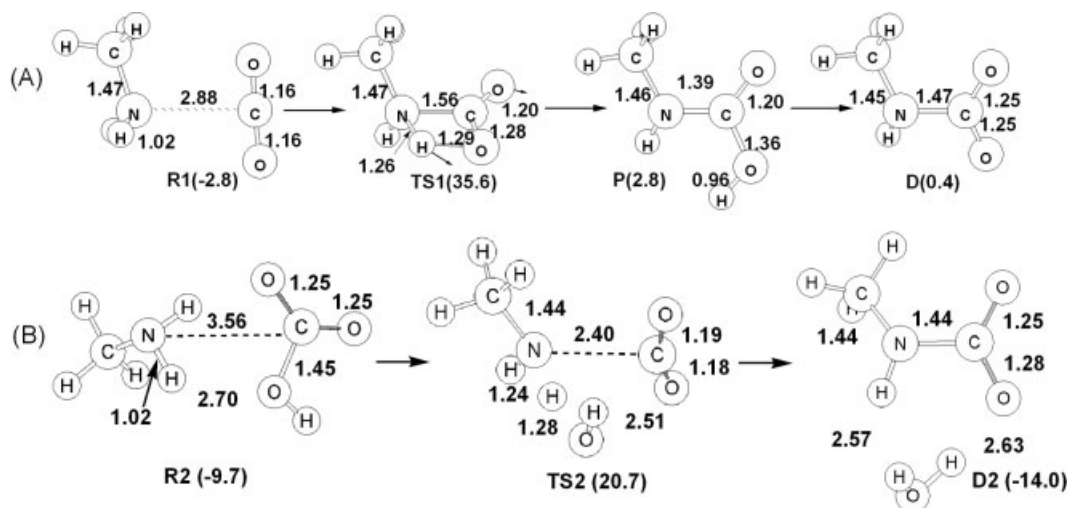
Fig. 1. Reactant complexes, transition states and products for methylamine carboxylation (**A**) by carbon dioxide and (**B**) by bicarbonate calculated at the B3LYP/6-31G(d,p) level of theory (key bond lengths in angstroms; energies without ZPE relative to isolated reactants in kilocalories per mole).

recent calculations found no evidence for such structures.[59]

Since our goal is to study lysine carboxylation in the active site of OXA-10, both carbon dioxide and bicarbonate have been considered in the reaction with methylamine. Reliable gas-phase experimental barrier heights are not available for either of these reactions. Hence high-level theoretical calculations have been carried out as a standard for comparison with lower levels of theory. In particular, the CBS–APNO method has been extensively tested and yields reliable geometries and accurate gas-phase energy differences (mean absolute deviation 0.5 kcal/mol).[38]

As shown in Figure 1, the reactants for the carboxylation of CH_3NH_2 by CO_2 form a weakly bound complex between neutral monomers, **R1**. The transition state, **TS1**, is rather high in energy, and the migrating hydrogen is roughly halfway along the reaction path. Similar structures have been found previously for this reaction.[56,60] During the course of the reaction in the protein, the carboxylated lysine is deprotonated. If bicarbonate is chosen as the proton acceptor, the gas-phase deprotonation reaction, $CH_3NHCO_2H + HCO_3^- \rightarrow CH_3NHCO_2^- + H_2O + CO_2$, (**P** $\rightarrow$ **D**) has a heat of reaction of -2.4 kcal/mol. The corresponding reaction transferring the proton to acetate is also slightly exothermic (-1.4 kcal/mol).

When bicarbonate is used to carboxylate methylamine, the gas-phase transition state, **TS2**, is significantly lower in energy than **TS1** relative to isolated reactants. The $HO-CO_2$ bond in the transition state has dissociated, and the resulting hydroxide abstracts a proton from methylamine to form $CH_3NHCO_2^- + H_2O$ as a product. Following the reaction path downhill from the transition state confirms that there are no additional transition states or intermediates along the path between the reactant complex **R2** and the product complex **D2**. The CBS–APNO calculated energies for the carboxylation reactions are compared to more cost-effective calculations in Table I.

TABLE I. Gas-Phase Enthalpies for CH_3NH_2 + CO_2 + HCO_3^- System†

Method	TS1[a]	TS2[b]	P[c]	D[d]
HF/6-31G(d)	54.3	37.0	6.8	6.4
MP2/6-31G(d)	38.3	22.6	8.0	3.7
B3LYP/6-31G(d)	35.3	22.8	4.6	5.6
B3LYP/6-31G(d,p)	33.5	21.2	3.1	4.1
B3LYP/6-311G(d,p)	37.8	18.1	6.4	3.3
CBS-APNO	35.6	20.7	2.8	0.4

†Enthalpies in kcal/mol at 298.15 K and 1 atm relative to CH_3NH_2 + CO_2 + HCO_3.
[a]addition of CO_2
[b]addition of HCO_3^-
[c]$CH_3NHCO_2H + HCO_3^-$
[d]$CH_3NHCO_2 + CO_2 + H_2O$

The Hartree–Fock (HF) method overestimates the barrier height significantly;[56] MP2 and B3LYP/6-311G(d,p) differ by 2–6 kcal/mol from the CBS–APNO results. Since density functional calculations reproduce the CBS–APNO relative energies quite well, the B3LYP/6-31G(d,p) level was chosen for the quantum region of the QM/MM calculations.

Carboxylation of Methylamine in Water

The mechanism of carboxylation of amines in solution is somewhat controversial.[49] Reaction orders between 1 and 2 in the amine have been observed. This has been interpreted as a competition between zwitterion formation and amine deprotonation. Alternatively, the rate data can be described equally well by a base-catalyzed carboxylation reaction in which either the amine or the solvent water can act as the base.[59] Calculations show that one or more molecules of water[59] or a second molecule of the amine[61] can assist in the proton transfer process and lower the barrier significantly. Explicit interaction with a molecule of water also calalyzes the hydrolysis of amides[62–69] and the hydration of CO_2[70,71] and carbonyls.[72–78]
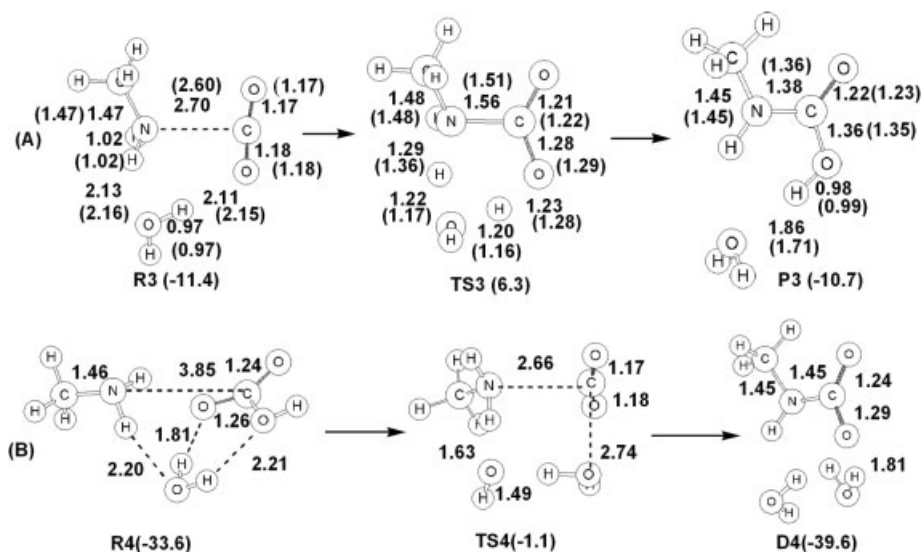
Fig. 2. Reactant complexes, transition states and products for water catalyzed methylamine carboxylation (**A**) by carbon dioxide and (**B**) by bicarbonate calculated at the B3LYP/6-31G(d,p) level of theory (key bond lengths in angstroms optimized in the gas phase; bond lengths in parentheses are optimized with CPCM solvent; gas energies relative to isolated reactants are in kilocalories per mole).

TABLE II. Energies for Carboxylation Reactions in QM/MM Models of Active Site for OXA-10 Compared to Gas-Phase and Solution[†]

Model	TS1	P	TS2	D	TS3	P3	TS4	D4
Gas phase	38.7	5.4	39.6	−1.0	17.7	0.7	32.5	−6.1
Solution	32.4	−5.6	37.4	−2.4	12.0	−10.6	36.6	−5.0
QM/MM	37.9	−12.0	25.6	−36.1	13.8	−12.7	42.8	−51.8

[†]Energies without ZPE in kcal/mol, computed at B3LYP/6-31G(d,p) relative to the corresponding reactant complexes.

Figure 2 shows the participation of H_2O in the carboxylation of methylamine by CO_2 and by HCO_3^-. A proton shifts from the water to the carbon dioxide or bicarbonate at the same time as the amine hydrogen moves to the water. The N—C and C—O bond lengths in the transition states **TS3** and **TS4** are nearly identical to the corresponding unassisted transition states, **TS1** and **TS2**. However, the barrier height for carboxylation by CO_2 is decreased much more by the catalytic water molecule (Table II, **TS3** vs. **TS1**) than the barrier height for HCO_3^- (**TS4** vs. **TS2**). Compared to the unassisted reaction for carboxylation by CO_2, the catalytic water molecule decreases the gas-phase barrier by 18 kcal/mol at the CBS–APNO level and 21 kcal/mol at B3LYP/6-31G(d,p). However, for carboxylation with bicarbonate, the catalytic water molecule decreases the barrier by only 7 kcal/mol.

Since zero-point energies are difficult to compute for QM/MM calculations on systems the size of OXA-10, Table II and Figures 1 and 2 list the energies without zero-point energy (ZPE) for the various reactions. Inclusion of ZPE decreases the barrier heights by 1–6 kcal/mol, but **TS3** is still 10–20 kcal/mol lower than the other transition states. In the active site, translation and rotation are very limited, but vibrational motion contributes to the entropy and to the free energy. The vibrational component of the free energy changes the barrier heights by less than 4 kcal/mol, and **TS3** remains the lowest transition state. Thus, the qualitative picture is the same when ZPE and vibrational entropy are considered – carboxylation with CO_2 assisted by a water molecule is preferred.

The effect of solvation by bulk water on the energy along the carboxylation reaction path can modeled using the CPCM self-consistent reaction field method. Table II lists the energies relative to the corresponding reactant clusters. For carboxylation of methylamine by carbon dioxide with and without catalysis by an explicit water molecule, **TS1** and **TS3**, modeling the bulk solvent causes a 6 kcal/mol decrease in the barrier compared to the gas phase. A barrier of 12 kcal/mol is calculated for **TS3**, in good agreement with the experimental activation energies of 9.2–13.0 kcal/mol obtained for the carboxylation of a variety of primary and secondary amines.[61,79−83] Solvation also stabilizes the protonated products **P** and **P3** by 10 kcal/mol. For carboxylation with bicarbonate, bulk solvent decreases the relative energy of the uncatalyzed transition state, **TS2**, and the deprotonated products, **D**, by only a small amount, but it increases the barrier by 4 kcal/mol in the presence of the catalytic water, **TS4**. In summary, the polarizable environment of the solvent lowers the energy the transition states and products relative to the reactant clusters for carboxylation by carbon dioxide but not for carboxylation by bicarbonate.

QM/MM Carboxylation of Lys-70 in OXA-10 β-Lactamase

The calculation of the carboxylation reactions in the gas phase and in solution provides a calibration for structures and energetics along a reaction path in the protein. The protein environment contributes to enzyme catalysis through electrostatic and steric interactions with the active site and substrate. In the QM/MM calculations, the portions of the structure relevant to the making and breaking of bonds in the transition structure are included in the quantum region. The C_δ, C_ϵ, and N_ζ atoms (and associated H atoms) of the Lys-70 side chain, as well as the atoms of the CO_2 or HCO_3^- molecule with and without a catalytic water, C_α, C_β, and O_γ of Ser-67, methylindole for the side chain of Trp-154, and a crystallographically conserved water molecule, were selected for the quantum region. The molecule of water that catalyzes the carboxylation by CO_2 was first observed in the active site during the equilibration step; its presence was confirmed in a 2-ns fully solvated molecular dynamics simulation, which revealed that a water molecule consistently occupies this site over the course of the trajectory. A radial distribution function between the carbamate oxygen and the water oxygen (shown in Fig. 2 in the Supplementary Material) further establishes the presence of this water molecule, as a large peak is observed around 2.8 Å. Figure 3 shows stereo views of the active site of the OXA-10 β-lactamase for the most promising pathway for carboxylation, water-assisted addition of CO_2 to Lys-70. Details of the structures are shown schematically in Figure 4.

For three of the four carboxylation reactions considered, the reactant complex, transition state, and product could be readily fitted into the active site. Table II lists the energies of the transition states and product complexes relative to the reactant complexes. For unassisted carboxylation by CO_2 or HCO_3^-, **TS1** and **TS2**, the barriers in QM/MM calculations are reduced from the gas phase, and are similar to or lower than those in solution. When a molecule of water assists the carboxylation by CO_2, the barrier for **TS3** is 14 kcal/mol. This pathway could also be reached by the interaction of bicarbonate with protonated Lys-70. The neutralization step involving a proton transfer from the protonated lysine to the bicarbonate should have no enthalpy barrier and yields a neutral Lys-70, CO_2, and a water molecule in position for the subsequent carboxylation step.

Various attempts to place **TS4** into the active site have encountered difficulties. In particular, there is not enough room for the catalytic water molecule. The hydroxyl group of Ser-67 is in a good position to participate in the proton relay between Lys-70 and the hydroxyl group of the bicarbonate, as shown in Figure 5. However, in this configuration only one of the two oxygens of the bicarbonate can hydrogen-bond to Trp-154 and the crystallographic water. Optimization of the transition state yields an N—C bond length that is longer than that of the unassisted bicarbonate transition state in the enzyme, but much shorter than that of **TS2** or **TS4** in the gas phase. The

resulting barrier is 5–10 kcal/mol higher than in the gas phase or solution calculations of **TS4**.

To summarize, the barrier for **TS3** is significantly lower than for **TS1**, **TS2**, or **TS4** in QM/MM calcuations. If bicarbonate is involved in the carboxylation reaction, it must first be neutralized so that the reaction can proceed via CO_2 and neutral Lys-70 catalyzed by a water molecule, **TS3**. The product complexes for all four pathways are stabilized significantly by the active-site environment, and the reactions are more exothermic than in the gas phase or in the model solvent. Since the transition state for the water-assisted carboxylation by CO_2, **TS3**, is significantly lower than for the other reactions, the discussion will concentrate on this pathway.

In the reactant complex, **QM/MM-R3** in Figure 4, the oxygen atoms of the CO_2 are hydrogen bonded to the side chain N of Trp-154 (2.93 Å), the crystallographically conserved water molecule (2.95 Å), and the catalytic water molecule (2.86 Å). The O_γ of Ser-67 is hydrogen bonded to the catalytic water (2.89 Å) and N_ζ of the Lys-70 side chain (2.96 Å). The O-C-O angle is 140°, and the distance between the N_ζ and the CO_2 carbon is 1.71 Å compared to 2.70 Å in the gas phase (**R3** in Fig. 2) and 2.60 Å in solution (**R3** optimized with the CPCM solvent model). This indicates the reactant complex has substantial amount of zwitterion character, and is supported by the Mulliken population analysis. The CO_2 group in **QM/MM-R3** has a charge of -0.29 compared to -0.55 for the carboxylate in **QM/MM-D**. In contrast to the gas phase, we were unable to find a reactant complex involving neutral groups. In the transition structure **QM/MM-TS3**, the catalytic water forms a six-membered ring with N and O of the carboxylated lysine. The shift of the proton from N to the catalytic water is more advanced than in the gas phase, but the transfer of the proton to the carboxylate oxygen is not as far along the reaction coordinate. When **TS3** was optimized with the CPCM solvent a similar effect was seen, but to a lesser degree. The O_γ of Ser-67 remains hydrogen bonded to the free hydrogen atom of the catalytic water (2.63 Å) but moves away from the side chain nitrogen of Lys-70 (3.90 Å) to make room for the catalytic water. The bond lengths in the product structure, **QM/MM-P3**, are very similar to those found in the gas phase calculations. Deprotonation of this structure leads to **QM/MM-D**, which is the most stable structure of this scheme; however, a good estimate of the actual energy difference is hard to obtain. If bicarbonate or acetate is chosen as the proton acceptor the reaction (**QM/MM-P3** + $HCO_3^- \rightarrow$ **QM/MM-D** + CO_2 + H_2O) is exothermic by 20.5 kcal/mol. The hydrogen bonding in **QM/MM-D** is similar to **QM/MM-P3**, involving Ser-67 (2.85 Å), Trp-154 (2.75 Å), the crystallographically conserved water molecule (2.77 Å) and the catalytic water molecule (2.69 Å).

In the X-ray structure, within the level of confidence inherent in the method (approx. 0.1 Å for 1.39 Å resolution structure of 1K55), the C—O bond lengths are equivalent (1.23 and 1.25 Å) and the N—C bond is 1.37 Å. This more closely resembles the bond lengths of the deprotonated product, **QM/MM-D**. The hydrogen-bond distances be-
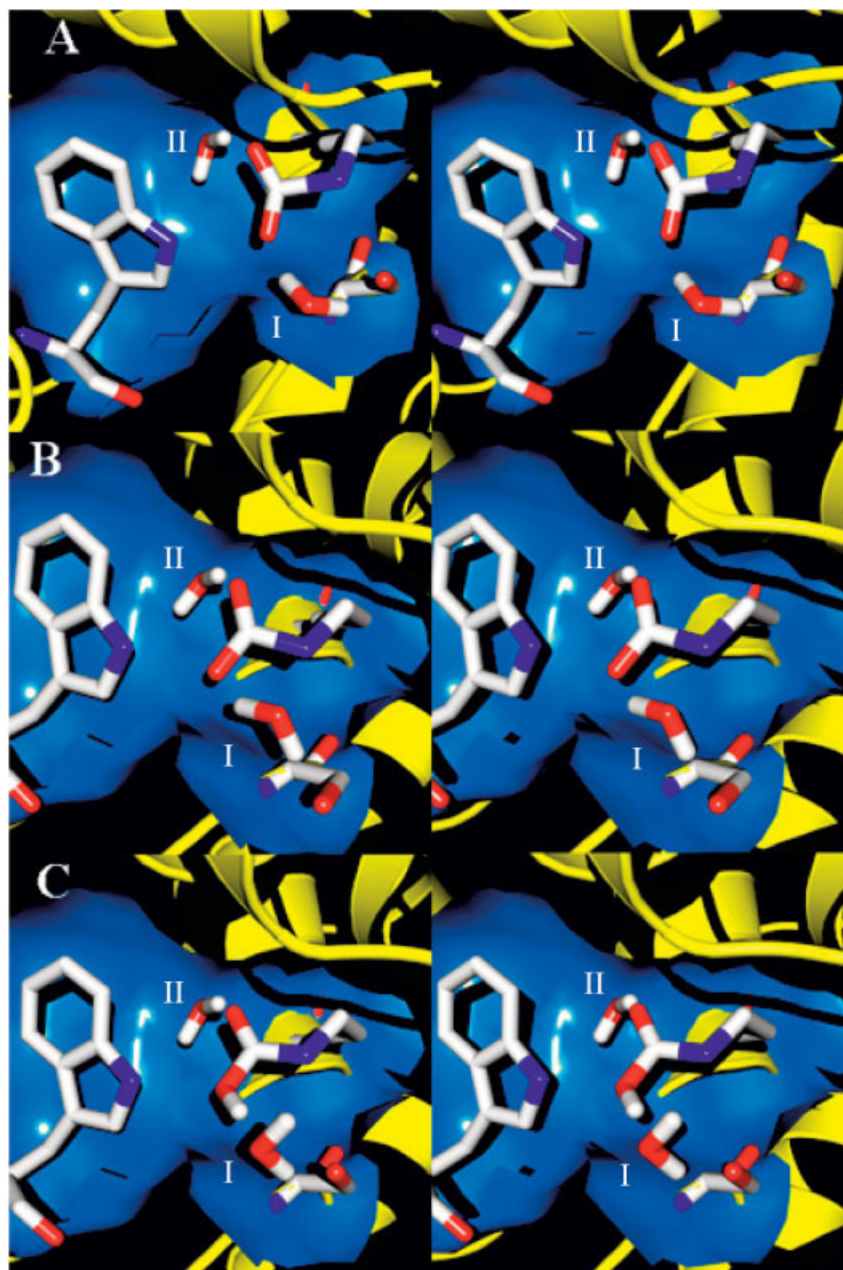
Fig. 3. Stereo view of the reactant, transition state, and product along the Lys-70 carboxylation reaction pathway. Atoms in the QM region are rendered in capped sticks and color-coded according to atom type (white, blue, and red correspond to carbon, nitrogen, and oxygen, respectively). These include carbon dioxide, the catalytic water molecule (labeled as I), C_γ, C_δ, and N_ζ of Lys-70, C_α, C_β, and O_γ of Ser-67, methylindole for the side chain of Trp-154 and a crystalograpically conserved water (labeled as II). The backbone of the OXA-10 β-lactamase is shown as a yellow ribbon. A solvent-accessible surface is constructed in blue around Lys-70. (**A**) Reactant species showing the complex formation of carbon dioxide and water with Lys-70. (**B**) Transition-state species showing the six-membered ring formation. (**C**) Product species showing carboxylated Lys-70 in its protonated form.

tween the carbamate nitrogen and Ser-67 (2.85 Å vs. 3.03 Å), and between the carbamate oxygen and the crystallographic water (2.77 Å vs. 2.78 Å) are also in good agreement. In the X-ray structure, the carbamate oxygen closest to Ser-67 is hydrogen bonded to the serine (2.72 Å) and to Trp-154 (2.98 Å). In the calculated structure, **QM/MM-D**, the distance from the carbamate oxygen to the Trp-154

nitrogen (2.71 Å) is similar to its X-ray value, but the space between the carbamate oxygen and O_γ of Ser-67 is occupied by the catalytic water. There are no crystallographically conserved water molecules adjacent to these atoms, but the X-ray structure shows that there is ample space close to these residues for water molecules to occupy. During the protein solvation step in preparation for
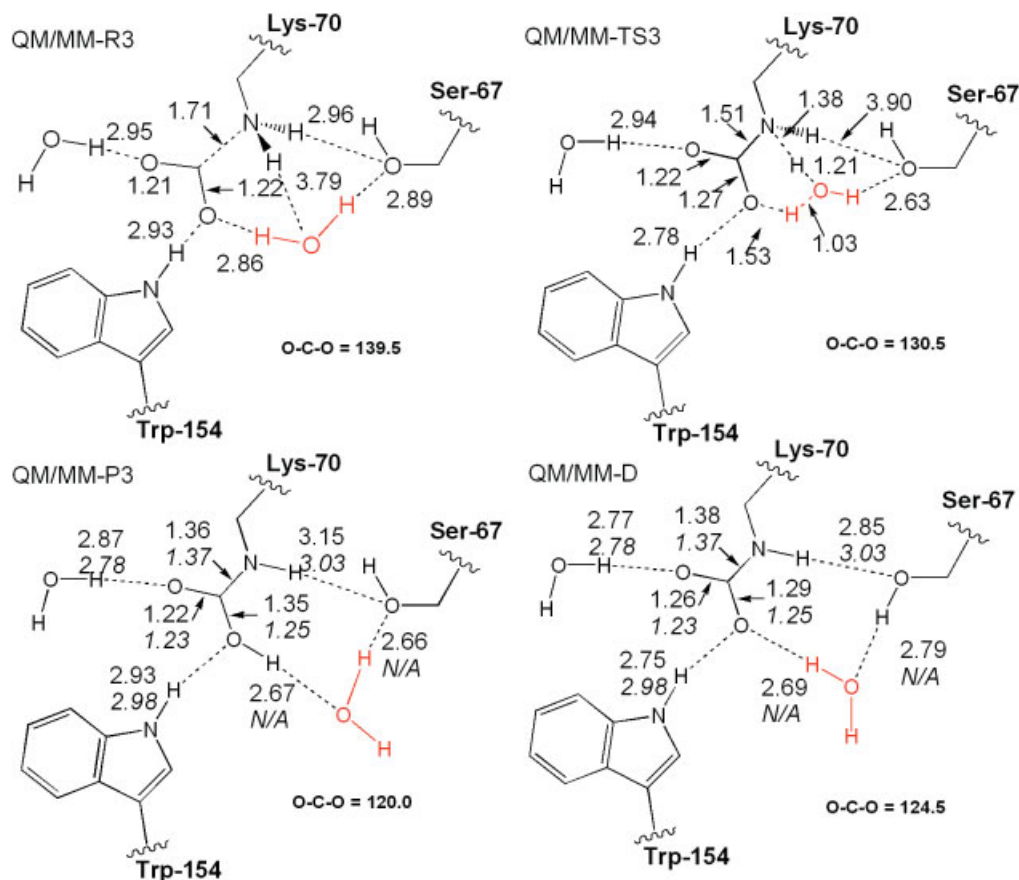
Fig. 4. Bond lengths (in angstroms) between heavy atoms in the OXA-10 β-lactamase active site carboxylation by CO_2 catalyzed by water. QM/MM-optimized geometries are in normal text; X-ray structure values are in italics; the catalytic water is in gray. [Color figure can be viewed in the online issue, which is available at www.interscience.wiley.com. The catalytic water is in red.]

QM/MM calculations, the system was fully immersed in a water box and subsequent molecular dynamics simulations enabled water molecules to equilibrate in the local active-site environment. One of these water molecules lies between the Trp-154, Ser-67, and Lys-70 residues. Over the course of the 2-ns dynamics simulation of the fully solvated carboxylated enzyme, a water molecule consistently occupied this site. In **QM/MM-D**, the Ser-67 hydroxyl hydrogen is bonded to this water molecule, while one of its hydrogen atoms is bonded to a carbamate oxygen atom (Fig. 4). Furthermore, kinetic data and X-ray structural information for a judiciously designed inhibitor with a hydroxyl group as a spatial surrogate for this water molecule recently documented its existence.[84] This water molecule not only assists in the carboxylation of lysine, but it also serves as the hydrolytic water molecule in the second step.[84]

To facilitate activation of Ser-67 for acylation by the substrate, its side-chain hydroxyl hydrogen must be transferred, and the active-site structure argues that the deprotonated Lys-70 carbamate is the best residue to receive this proton. While the X-ray structure shows a direct contact between the side chains of Ser-67 and Lys-70 carbamate, the calculations indicate there is an interven-

ing molecule of water. This is the water molecule that assists the lysine carboxylation reaction, and it remains hydrogen bonded to the Lys-70 carbamate oxygen and the Ser-67 hydroxyl (Figs. 3 and 4). The orientation of the hydrogen atoms in this network suggests that the activation of Ser-67 for the acylation step could occur by proton transfer through this hydrogen-bonded water molecule rather than directly to the carbamate oxygen. The implication of our finding is that the carboxylated lysine promotes Ser-67 for the acylation via this intervening water molecule. This very same water molecule—seen in the dynamics simulation but not observed in the X-ray structure—is the proposed hydrolytic water molecule that is also activated by carboxylate lysine for the second step of catalysis, the deacylation of the acyl-enzyme species.[84] The X-ray structure of the OXA-10 β-lactamase acylated by 7β-hydroxypropylpenicillanate is revealing in this respect.[84] This structure showed that on acylation, the hydroxyl of the 7β moiety occupied the space that the water molecule would occupy within the active site; in essence, it replaced it. This acyl-enzyme species was devoid of ability to undergo the second step (deacylation) of the enzymic catalysis. Hence, we deduce that the same water molecule is intimately involved in both active-site acylation and
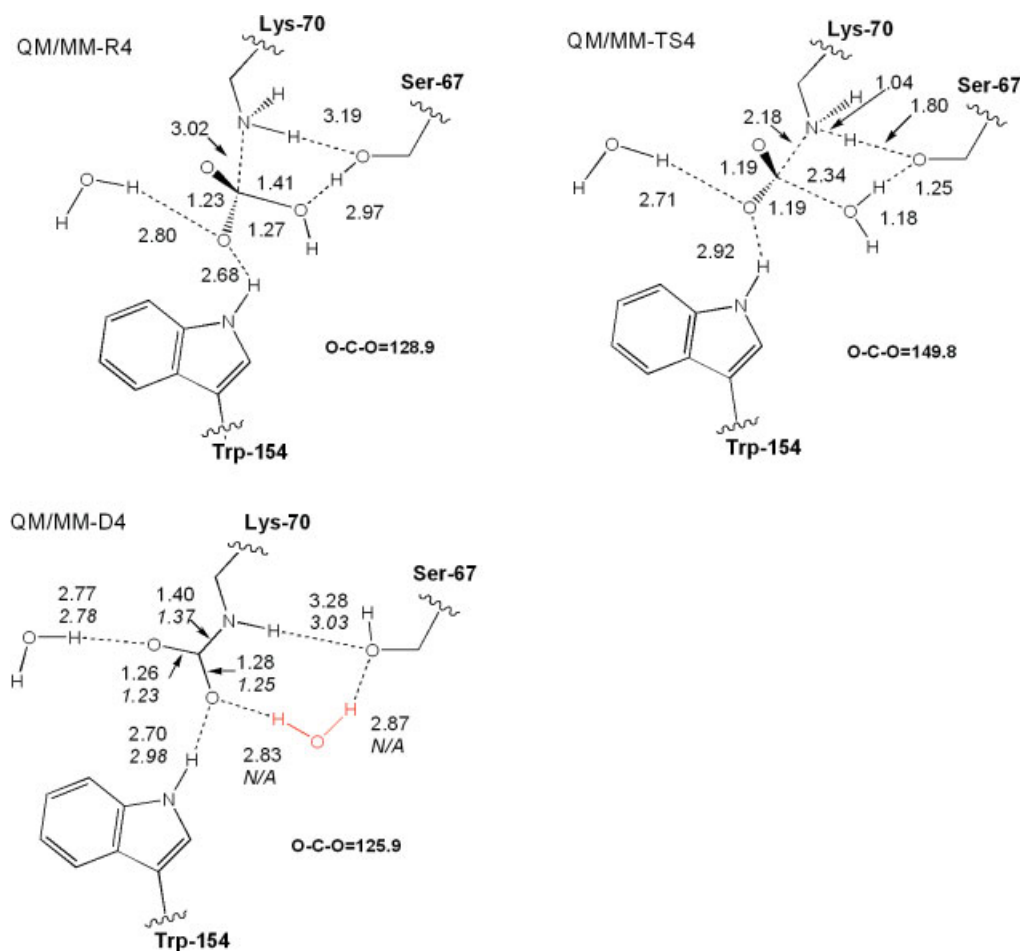
Fig. 5. Bond lengths (in angstroms) between heavy atoms in the OXA-10 β-lactamase active site carboxylation by HCO_3^- catalyzed by water. QM/MM optimized geometries are in normal text; X-ray structure values are in italics; the catalytic water is in gray. [Color figure can be viewed in the online issue, which is available at www.interscience.wiley.com. The catalytic water is in red.]

deacylation chemistries, as well as in the carboxylation step.

At pH 7.0, the OXA-10 β-lactamase exhibits biphasic kinetics for a number of β-lactam substrates.[16] This could be due to decarboxylation of the lysine carbamate partway through catalytic turnover. For catalysis to resume, the enzyme must experience recarboxylation, hence the slower second step. Protonation of the lysine carbamate is a necessary step in decarboxylation. Decarboxylation via protonation at one of the terminal carbamate oxygen atoms encounters a barrier of more than 30 kcal/mol, which is essentially the reverse of the reaction path studied above. However, previous calculations show that protonation at the carbamate nitrogen atom leads to a barrierless decarboxylation reaction.[7] The latter case provides a scenario in which removal of a proton from Ser-67 to activate it for enzyme acylation could lead to decarboxylation via protonation of the carbamate nitrogen and formation of an inactive enzyme in mid-catalysis. For the enzyme to complete its catalytic cycle, the lysine would need to be carboxylated again, giving rise to the biphasic kinetics observed for OXA-10 β-lactamase with some

substrates. This finding is consistent with the experimental observation that supplementation of the reaction medium with excess bicarbonate, as a source of carbon dioxide, simplifies the kinetics to a monophasic process by readily facilitating recarboxylation of the lysine residue.[16]

CONCLUSIONS

The QM/MM calculations show that the carboxylation reaction changes from endothermic in the gas phase to exothermic in the enzyme, demonstrating that the carboxylated lysine is stabilized by the active site. A water molecule in the active site participates in a proton shuttle, lowering the barrier to approximately 14 kcal/mol. The deprotonated lysine carbamate structure exhibits additional stabilization within the enzyme environment, suggesting that it is the most stable species of those investigated. Of the various structures on the reaction path, the deprotonated product most closely resembles the X-ray crystal structure. Therefore, we propose that the deprotonated lysine carbamate is the active species observed in the X-ray crystal structure. The water molecule that catalyzes the first step is likely also to be involved in the

acylation and deacylation steps. The proton transfer for activation of Ser-67, the acylation reaction, and the subsequent deacylation of the enzyme–substrate complex are beyond the scope of this work, and will be followed up subsequently. The biphasic kinetics observed for the OXA-10 β-lactamase can be explained by a barrierless decarboxylation through a protonation on the carbamate nitrogen atom.

Carboxylation of lysine enriches the side chain functionalities of the twenty normal amino acids and may be more widespread than previously thought. Carboxylation is favored when the lysine sits in a hydrophobic pocket that lowers its pK_a and when the local environment stabilizes the deprotonated carbamate. Processes similar to those discussed above may hold for other enzymes that incorporate carboxylated lysine in their structures.

ACKNOWLEDGMENTS

REFERENCES

1. Jabri E, Carr MB, Hausinger RP, Karplus PA. The crystal structure of urease from *Klebsiella aerogenes*. Science 1995; 268(5213):998–1004.
2. Benning MM, Kuo JM, Raushel FM, Holden HM. Three-dimensional structure of the binuclear metal center of phosphotriesterase. Biochemistry 1995;34(25):7973–7978.
3. Shibata N, Inoue T, Fukuhara K, Nagara Y, Kitagawa R, Harada S, Kasai N, Uemura K, Kato K, Yokota A, Kai Y. Orderly disposition of heterogeneous small subunits in D-ribulose-1,5-bisphosphate carboxylase/oxygenase from spinach. J Biol Chem 1996;271(43):26449–26452.
4. Maveyraud L, Golemi D, Kotra LP, Tranier S, Vakulenko S, Mobashery S, Samama JP. Insights into class D beta-lactamases are revealed by the crystal structure of the OXA10 enzyme from *Pseudomonas aeruginosa*. Structure Fold Des 2000;8(12):1289–1298.
5. Golemi-Kotra D, Cha JY, Meroueh SO, Vakulenko SB, Mobashery S. Resistance to beta-lactam antibiotics and its mediation by the sensor domain of the transmembrane BlaR signaling pathway in *Staphylococcus aureus*. J Biol Chem 2003;278(20):18419–18425.
6. Sun T, Nukaga M, Mayama K, Braswell EH, Knox JR. Comparison of beta-lactamases of classes A and D: 1.5-Å crystallographic structure of the class D OXA-1 oxacillinase. Prot Sci 2003;12(1):82–91.
7. Birck C, Cha JY, Cross J, Schulze-Briese C, Meroueh SO, Schlegel HB, Mobashery S, Samama JP. X-ray crystal structure of the acylated beta-lactam sensor domain of BlaR1 from *Staphylococcus aureus* and the mechanism of receptor activation for signal transduction. J Am Chem Soc 2004;126:13945–13947.
8. Bush K, Mobashery S. How beta-lactamases have driven pharmaceutical drug discovery. From mechanistic knowledge to clinical circumvention. Adv Exp Med Biol 1998;456:71–98.
9. Kotra LP, Samama JP, Mobashery S. Structural aspects of β-lactamase evolution. In: Lewis A, Salyers AA, Haber H, Wax RG, editors. Bacterial resistance to antimicrobials, mechanisms, genetics, medical practice and public health. New York: Marcel Dekker, Inc.; 2002. p 123–159.
10. Lorimer GH, Badger MR, Andrews J. Rubisco carboxylation of lysine. Biochemistry 1976;15:529–536.
11. Shim H, Raushel FM. Self-assembly of the binuclear metal center of phosphotriesterase. Biochemistry 2000;39(25):7357–7364.
12. Thoden JB, Phillips GN, Jr., Neal TM, Raushel FM, Holden HM. Molecular structure of dihydroorotase: a paradigm for catalysis through the use of a binuclear metal center. Biochemistry 2001; 40(24):6989–6997.
13. Morollo AA, Petsko GA, Ringe D. Structure of a Michaelis complex analogue: propionate binds in the substrate carboxylate site of alanine racemase. Biochemistry 1999;38(11):3293–3301.
14. Golemi-Kotra D, Meroueh SO, Kim C, Vakulenko SB, Bulychev A, Stemmler AJ, Stemmler TL, Mobashery S. The importance of a critical protonation state and the fate of the catalytic steps in class A beta-lactamases and penicillin-binding proteins. J Biol Chem 2004;279(33):34665–34673.
15. Oliva M, Dideberg O, Field MJ. Understanding the acylation mechanisms of active-site serine penicillin-recognizing proteins: A molecular dynamics simulation study. Proteins 2003;53(1):88–100.
16. Golemi D, Maveyraud L, Vakulenko S, Samama JP, Mobashery S. Critical involvement of a carbamylated lysine in catalytic function of class D beta-lactamases. Proc Natl Acad Sci USA 2001;98(25): 14280–14285.
17. Tien M, Berlett BS, Levine RL, Chock PB, Stadtman ER. Peroxynitrite-mediated modification of proteins at physiological carbon dioxide concentration: pH dependence of carbonyl formation, tyrosine nitration, and methionine oxidation. Proc Natl Acad Sci USA 1999;96(14):7809–7814.
18. Paetzel M, Danel F, de Castro L, Mosimann SC, Page MG, Strynadka NC. Crystal structure of the class D beta-lactamase OXA-10. Nat Struct Biol 2000;7(10):918–925.
19. Danel F, Frere JM, Livermore DM. Evidence of dimerisation among class D beta-lactamases: kinetics of OXA-14 beta-lactamase. Biochim Biophys Acta 2001;1546(1):132–142.
20. Gao J. Methods and applications of combined quantum mechanical and molecular mechanical potentials. In: Lipkowitz KB, Boyd DB, editors. Reviews in computational chemistry, vol. 7. New York: VCH; 1996. p 119–185.
21. Froese RDJ, Morokuma K. Hybrid methods. In: Schleyer PvR, Allinger NL, Kollman PA, Clark T, Schaefer III HF, Gasteiger J, Schreiner PR, editors. Encyclopedia of computational chemistry, vol. 2. Chichester: Wiley; 1998. p 1244–1257.
22. Monard G, Merz KM. Combined quantum mechanical/molecular mechanical methodologies applied to biomolecular systems. Acc Chem Res 1999;32(10):904–911.
23. Torrent M, Vreven T, Musaev DG, Morokuma K, Farkas O, Schlegel HB. Effects of the protein environment on the structure and energetics of active sites of metalloenzymes. ONIOM study of methane monooxygenase and ribonucleotide reductase. J Am Chem Soc 2002;124(2):192-193.
24. Maseras F, Morokuma K. Imomm - a new integrated ab initio + molecular mechanics geometry optimization scheme of equilibrium structures and transition states. J Comput Chem 1995;16(9): 1170–1179.
25. Dapprich S, Komaromi I, Byun KS, Morokuma K, Frisch MJ. A new ONIOM implementation in Gaussian98. Part I. The calculation of energies, gradients, vibrational frequencies and electric field derivatives. J Mol Struct-THEOCHEM 1999;462:1–21.
26. Vreven T, Morokuma K. Investigation of the $S_0 \ S_1$ excitation in bacteriorhodopsin with the ONIOM(MO:MM) hybrid method. Theor Chem Acc 2003;109:125–132.
27. Frisch MJ, Trucks GW, Schlegel HB, Scuseria GE, Robb MA, Cheeseman JR, Montgomery JA, Vreven T, Kudin KN, Burant JC, Millam JM, Iyengar S, Tomasi J, Barone V, Mennucci B, Cossi M, Scalmani G, Rega N, Petersson GA, Ehara M, Toyota K, Hada M, Fukuda R, Hasegawa J, Ishida M, Nakajima T, Kitao O, Nakai H, Honda Y, Nakatsuji H, Li X, Knox JE, Hratchian HP, Cross JB, Adamo C, Jaramillo J, Cammi R, Pomelli C, Gomperts R, Stratmann RE, Ochterski J, Ayala PY, Morokuma K, Salvador P, Dannenberg JJ, Zakrzewski VG, Dapprich S, Daniels AD, Strain MC, Farkas Ö, Malick DK, Rabuck AD, Raghavachari K, Foresman JB, Ortiz JV, Cui Q, Baboul AG, Clifford S, Cioslowski J, Stefanov BB, Liu G, Liashenko A, Piskorz P, Komaromi I, Martin RL, Fox DJ, Keith T, Al-Laham MA, Peng CY, Nanayakkara A, Challacombe M, Gill PMW, Johnson B, Chen W, Wong MW, Andres JL, Gonzalez C, Head-Gordon M, Replogle ES, Pople JA. Gaussian 01, Development Version (Revision B.02). Revision B.02. Pittsburgh, PA: Gaussian, Inc.; 2002.
28. Roothan CCJ. New developments in molecular orbital theory. Rev Mod Phys 1951;23:69–89.
29. Moller C, Plesset MS. Note on the approximation treatment for many-electron system. Phys Rev 1934;46:618–622.
30. Pople JA, Seeger R, Krishnan R. Variational configuration interac-

tion methods and comparison with perturbation theory. Int J Quantum Chem 1977;11:149–163.

31. Becke AD. Density-functional exchange-energy approximation with correct asymptotic behavior. Phys Rev A 1988;38(6):3098–3100.

32. Becke AD. Density-functional thermochemistry. 3. The role of exact exchange. J Chem Phys 1993;98(7):5648–5652.

33. Lee CT, Yang WT, Parr RG. Development of the Colle-Salvetti correlation-energy formula into a functional of the electron-density. Phys Rev B 1988;37:785–789.

34. Ditchfield R, Hehre WJ, Pople JA. Self-consistent molecular-orbital methods. IX. Extended Gaussian-type basis for molecular-orbital studies of organic molecules. J Chem Phys 1971;54:724–728.

35. Hariharan PC, Pople JA. Influence of polarization functions on MO hydrogenation energies. Theor Chim Acta 1973;28:213–222.

36. Mclean AD, Chandler GS. Contracted Gaussian basis sets for molecular calculations. I. Second row atoms, Z = 11-18. J Chem Phys 1980;72:5639–5648.

37. Krishnan R, Binkley JS, Seeger R, Pople JA. Self-consistent molecular orbital methods. XX. A basis set for correlated wave functions. J Chem Phys 1980;72:650–654.

38. Montgomery JA, Ochterski J, Petersson GA. A complete basis set model chemistry. IV. An improved atomic pair natural orbital method. J Chem Phys 1994;101:5900–5909.

39. Pople JA, Head-Gordon M, Raghavachari K. Quadratic configuration-interaction - a general technique for determining electron correlation energies. J Chem Phys 1987;87(10):5968–5975.

40. Barone V, Cossi M. Quantum calculation of molecular energies and energy gradients in solution by a conductor solvent model. J Phys Chem A 1998;102(11):1995–2001.

41. Tripos I. Sybyl 6.7. 1699 Sourth Hanley Rd., St. Louis, Missouri, 63144, USA.

42. Case DA, Pearlman DA, Caldwell JW, Cheatham III TE, Ross WS, Simmerling CL, Darden TA, Merz KM, Seibel GL, Cheng AL. AMBER 6. San Francisco: University of California; 1999.

43. Wang J, Cieplak P, Kollman PA. How well does a restrained electrostatic potential (RESP) model perform in calculating conformational energies of organic and biological molecules? J Comput Chem 2000;21:1049–1074.

44. Bayly CI, Cieplak P, Cornell WD, Kollman PA. A well-behaved electrostatic potential based method using charge restraints for deriving atomic charges - the RESP model. J Chem Phys 1993;97:10269–10280.

45. Darden T, York D, Pedersen L. Particle Mesh Ewald - an N.Log(N) method for Ewald sums in large systems. J Chem Phys 1993;98(12):10089–10092.

46. Ryckaert J-P, Ciccotti G, Berendsen HJC. Numerical integration of the Cartesian equations of motion of a system with constraints: molecular dynamics of n-alkanes. J Comput Phys 1977;23(3):327–341.

47. Vreven T, Morokuma K, Farkas O, Schlegel HB, Frisch MJ. Geometry optimization with QM/MM, ONIOM, and other combined methods. I. Microiterations and constraints. J Comput Chem 2003;24:760–769.

48. Kollman PA, Dixon R, Cornell WD, Fox T, Chipot C, Pohorille A. The development/application of a minimalist molecular mechanics force field using a combination of ab initio calculations and experimental data. In: Wilkinson A, Weiner P, van Gunsteren W, editors. Computation simulations of biomolecular systems, vol. 3. New York: Elsevier; 1997. p 83–96.

49. Dell'Amico DB, Calderazzo F, Labella L, Marchetti F, Pampaloni G. Converting carbon dioxide into carbamato derivatives. Chem Rev 2003;103(10):3857–3897.

50. Camacho F, Sanchez S, Pacheco R. Absorption of carbon dioxide at high partial pressures in 1-amino-2-propanol aqueous solution. Considerations of thermal effects. Ind Eng Chem Res 1997;36(10):4358–4364.

51. Suda T, Iwaki T, Mimura T. Facile determination of dissolved species in CO2-amine-H2O system by NMR spectroscopy. Chem Lett 1996(9):777-778.

52. Xu S, Wang YW, Otto FD, Mather AE. Kinetics of the reaction of carbon dioxide with 2-amino-2-methyl-1-propanol solutions. Chem Eng Sci 1996;51(6):841–850.

53. Saha AK, Bandyopadhyay SS, Biswas AK. Kinetics of absorption of CO2 into aqueous-solutions of 2-amino-2-methyl-1-propanol. Chem Eng Sci 1995;50(22):3587–3598.

54. Hagewiesche DP, Ashour SS, Alghawas HA, Sandall OC. Absorption of carbon dioxide into aqueous blends of monoethanolamine and N-methyldiethanolamine. Chem Eng Sci 1995;50(7):1071–1079.

55. Rinker EB, Ashour SS, Sandall OC. Kinetics and modelling of carbon dioxide absorption into aqueous solutions of N-methyldiethanolamine. Chem Eng Sci 1995;50(5):755–768.

56. Andres J, Moliner V, Krechl J, Silla E. A theoretical study of the addition mechanism of carbon dioxide to methylamine – modeling CO_2-biotin fixation. J Chem Soc Perkin Trans 2 1993(3):521–523.

57. Benitezgarcia J, Ruizibanez G, Alghawas HA, Sandall OC. On the effect of basicity on the kinetics of CO_2 absorption in tertiary amines. Chem Eng Sci 1991;46(11):2927–2931.

58. Andres J, Bohm S, Moliner V, Silla E, Tunon I. A theoretical study of stationary structures for the addition of azide anion to tetro-furanosides: modeling the kinetic and thermodynamic controls by solvent effects. J Phys Chem 1994;98(28):6955–6960.

59. da Silva EF, Svendsen HF. Ab initio study of the reaction of carbamate formation from CO_2 and alkanolamines. Ind Eng Chem Res 2004;43(13):3413–3418.

60. Andres J, Moliner V, Krechl J, Silla E. A theoretical study of the effect of basis sets on stationary structures for the addition of carbon-dioxide to methylamine: a relation among geometries, energy status, and electronic structures. Int J Quantum Chem 1993;45(5):433–444.

61. Jamroz MH, Dobrowolski JC, Borowiak MA. Ab initio study on the 1:2 reaction of CO_2 with dimethylamine. J Mol Struct 1997;404(1-2):105–111.

62. Williams IH. Theoretical modeling of specific solvation effects upon carbonyl addition. J Am Chem Soc 1987;109(21):6299–6307.

63. Lledos A, Bertran J. Lactam-lactim tautomeric interconversion mechanism of 2-pyridone in aqueous solution. Tetra Lett 1981;22(8):775–778.

64. Lledos A, Bertran J, Ventura ON. Water-chain intervention in the ketonization of vinyl alcohol. An ab initio study. Int J Quantum Chem 1986;30(4):467–477.

65. Ventura ON, Lledos A, Bonaccorsi R, Bertran J, Tomasi J. Theoretical study of reaction mechanisms for the ketonization of vinyl alcohol in gas phase and aqueous solution. Theor Chem Acta 1987;72(3):175–195.

66. Clavero C, Duran M, Lledos A, Ventura ON, Bertran J. Theoretical study of the addition of hydrogen halides to olefins: a comparison between $(HCl)_2$ and $(HF)_2$ additions to ethylene. J Comput Chem 1987;8(4):481–488.

67. Nguyen MT, Hegarty AF. Ab initio study of the hydration of ketenimine (CH_2=C—NH) by water and water dimer. J Am Chem Soc 1983;105(12):3811–3815.

68. Nguyen MT, Hegarty AF. Molecular orbital study on the hydrolysis of ketene by water dimer: .beta.-carbon vs oxygen protonation. J Am Chem Soc 1984;106(6):1552–1557.

69. Antonczak S, Ruizlopez MF, Rivail JL. Ab initio analysis of water-assisted reaction mechanisms in amide hydrolysis. J Am Chem Soc 1994;116(9):3912–3921.

70. Pocker Y, Bjorkquist DW. Stopped-flow studies of carbon dioxide hydration and bicarbonate dehydration in water and water-d2. Acid-base and metal ion catalysis. J Am Chem Soc 1977;99(20):6537–6543.

71. Palmer DA, Vaneldik R. The chemistry of metal carbonato and carbon-dioxide complexes. Chem Rev 1983;83(6):651–731.

72. Williams IH, Spangler D, Femec DA, Maggiora GM, Schowen RL. Theoretical models for transition-state structure and catalysis in carbonyl addition. J Am Chem Soc 1980;102(21):6619–6621.

73. Williams IH, Spangler D, Femec DA, Maggiora GM, Schowen RL. Theoretical models for solvation and catalysis in carbonyl addition. J Am Chem Soc 1983;105(1):31–40.

74. Nguyen MT, Ha TK. A theoretical study of the formation of carbonic acid from the hydration of carbon dioxide: a case of active solvent catalysis. J Am Chem Soc 1984;106(3):599–602.

75. Ruelle P. Ab initio study of the unimolecular pyrolysis mechanisms of formic-acid: additional comments based on refined calculations. J Am Chem Soc 1987;109(7):1722–1725.

76. Ruelle P, Kesselring UW, Namtran H. Ab initio quantum-chemical study of the unimolecular pyrolysis mechanisms of formic acid. J Am Chem Soc 1986;108(3):371–375.

77. Buckingham AD, Handy NC, Rice JE, Somasundram K, Dijkgraaf C. Reactions involving CO_2, H_2O, and NH_3 - the formation of (I)

carbamic acid, (II) urea, and (III) carbonic-acid. J Comput Chem 1986;7(3):283–293.

78. Ventura ON, Coitino EL, Lledos A, Bertran J. Analysis of the gas-phase addition of water to formaldehyde: a semiempirical and ab initio study of bifunctional catalysis by H2O. J Comput Chem 1992;13(9):1037–1046.

79. Caplow M. Kinetics of carbamate formation and breakdown. J Am Chem Soc 1968;90:6795–6803.

80. Danckwerts PV, Sharma MM. The absorption of carbon dioxide into solutions of alkalis and amines. Ind Eng 1966;10:CE244.

81. Hikita H, Asai S, Ishidkawa H, Honda M. The kinetics of reactions of carbon dioxide with monoethanolamine, diethanolamine and triethanolamine by a rapid mixing method. Chem Eng J 1977;13: 7–12.

82. Leder F. The absorption of CO_2 into chemically reactive solutions at high temperatures. Chem Eng Sci 1971;26(9):1381–1390.

83. Nunge RJ, WGill WN. Gas-liquid kinetics: the absorption of carbon dioxide in diethanolamine. AIChE J 1963;9:469–474.

84. Maveyraud L, Golemi-Kotra D, Ishiwata A, Meroueh O, Mobashery S, Samama JP. High-resolution X-ray structure of an acyl-enzyme species for the class D OXA-10 beta-lactamase. J Am Chem Soc 2002;124(11):2461–2465.